CrossMark

Increased Oxidative DNA Damage in Placenta Contributes to Cadmium-Induced Preeclamptic Conditions in Rat

Xiaojie Zhang[1] · Zhangye Xu[2] · Feng Lin[1] · Fan Wang[2] · Duyun Ye[3] · Yinping Huang[1]

Abstract To explore the possible mechanisms of cadmium (Cd)-induced preeclamptic conditions in rats. In the present study, we introduced the in vivo model of preeclampsia by giving intraperitoneal injections of cadmium chloride ($CdCl_2$) to pregnant rats from gestational day (GD) 4 to 19. Maternal body weights were recorded on GD 0, 14, and 20, while their systolic blood pressures (SBPs) monitored on GD 3, 11, and 18. On GD 20, rats were sacrificed and the specimens were collected. The morphological changes of placenta and kidney tissues of pregnant rats were examined by hematoxylin and eosin staining assay. Blood Cd level was detected by inductively coupled plasma mass spectrometry. Total antioxidant capacity (TAC) was evaluated using FRAP method and total nitrite (NOx) was detected with Griess reagent. Antioxidative factors and DNA damage/repair biomarkers were measured by real-time qPCR, western blot or immunohistochemistry study. The current results showed that $CdCl_2$-treated pregnant rats developed preeclampsia (PE)-like manifestations, such as hypertension, albuminuria, with decreased TAC and increased blood Cd level, and pro-oxidative/antioxidative or DNA damage/repair biomarkers. Our study demonstrated that increased oxidative DNA damage in placenta could contribute to Cd-induced preeclamptic conditions in rat.

✉ Yinping Huang
  yphuangp@126.com

[1] Department of Gynecology and Obstetrics, The First Affiliated Hospital of Wenzhou Medical University, Wenzhou 325000, China

[2] Department of Gynecology and Obstetrics, The Second Affiliated Hospital of Wenzhou Medical University, Wenzhou 325000, China

[3] Department of Pathophysiology, Tongji Medical College, Huazhong University of Science and Technology, Wuhan 430030, China

Introduction

Preeclampsia (PE) is a multisystemic disorder which is unique to human pregnancy, affecting 3–5 % of pregnant women and being one of the most serious complications of pregnancy [1]. The past decades have witnessed a large armamentaria of in vivo and in vitro investigations extensively and intensively launched out in an attempt to unveil the causative factors and explore the pathophysiological mechanisms of the disorder; the exact etiology of PE remains obscure [2].

As one of the toxic elements and environmental pollutants, cadmium (Cd) is reported to have a relationship with human PE, and its toxic effects share strikingly similar features to many of the clinical manifestations of PE, such as hypertension, proteinuria, fetal growth restriction (FGR), decreased placental perfusion, vasoconstriction, maternal-fetal immune intolerance, convulsions, liver, and renal lesions, but the underlying mechanisms is still a mystery [3, 4].

The most conclusive evidence that links Cd with hypertensive disorders came from an animal experiment launched in 1965, which gave rise to the successful replication of the toxemia model by injecting pregnant rats with the aqueous solution of Cd. Those scholars suggested that the presence of functioning placenta tissue may be a prerequisite for the bioeffects of Cd to be exerted [3]. Despite of the precedent achievement of the PE animal model induced by $CdCl_2$, the exact mechanism has yet to be clarified. Therefore, the current study focuses on the exploration of the possible pathophysiological mechanisms of the in vivo model of PE induced by Cd in pregnant rats.

Materials and Methods

Animals

Adult Sprague–Dawley female rats, 8–10 weeks old and weighing 220–250 g, were purchased from the Experimental Animal Center of Tongji Medical College, Huazhong University of Science and Technology (Wuhan, China), for studies approved by the Animal Care and Use Committee of Tongji Medical College. Animals were housed individually in cages with sterilized wood chips as bedding and maintained under pathogen-free conditions with controlled temperature (22–25 °C), humidity (50–60 %), and a 12-h light and dark cycle. Standard laboratory chows and tap water were available ad libitum to the rats. The cycling female rats with normal basic systolic blood pressure (SBP) (82–120 mmHg) were mated with male rats overnight. The next morning, a visible vaginal plug or detection of sperms in vaginal smear was confirmed as a sign of conception and that day was defined day 0 of gestation (GD 0).

Experimental Designs and Treatments

Pregnant rats were randomly assigned into three groups: the 0.5 Cd group ($n = 8$), the 0.25 Cd group ($n = 10$), and the control group ($n = 10$). At the same time, 12 virgin female rats with normal basic SBP were divided into two groups: the 0.5 Cd non-pregnant (NP) group ($n = 6$) and the 0.25 Cd NP group ($n = 6$). $CdCl_2$ (Sigma-Aldrich, USA) was dissolved in saline, and pregnant rats were injected intraperitoneally with the dose of 0.5, 0.25, and 0 mg Cd/kg b.w./day in a total application volume of 2 ml/kg b.w. from GD 4 to 19, respectively, while the NP groups received the corresponding dose of $CdCl_2$ solution consecutively for 16 days.

Methods

Systolic Blood Pressure Measurement

SBPs of pregnant rats were measured in the morning on GD 3, 11, and 18, regularly, with the NP groups being measured at the same time point. Indirect SBP monitoring was achieved with the tail cuff and pressure transducer connected to an automatic recorder system (BP-98A, Softron, Japan).

Specimen Collection

Pregnant rats were sacrificed on GD 20 under anesthetized conditions (10 % chloral hydrate, 350 mg/kg b.w., i.p.), and their pups were delivered by cesarean section. Blood specimens were obtained by heart puncture while urine samples, vesicopuncture. After centrifuged, sera and supernatants of urine specimens were stored at −80 °C for further assessments. Three placentae and one kidney were randomly selected from each pregnant rat and fixed in 10 % neutral buffered formalin for hematoxylin and eosin (HE) staining analysis or 4 % paraformaldehyde solution for immunohisto-chemistry study. The remainders were stored at −80 °C and allocated to real-time qPCR, western blot, or other biochemical assays.

Urinary Protein Quantification

Urine samples were thawed and recovered to room temperature before analyses. After specimens were diluted, the protein concentrations were quantified by a BCA protein assay kit (Pierce, Rockford, Illinois, USA) using bovine serum albumin (BSA) as a standard. All procedures were carried out according to the manufacturer's instructions.

Determination of Cadmium Concentration

Cd in maternal blood was measured by inductively coupled plasma mass spectrometry (ICP-MS) (Agilent 7500 with a Cd program, USA) with a detection limit of 15 μg/L for blood samples.

Nitrite (NO_2)/Nitrate (NO_3) Production Measurement

Accumulations of NO_2 and NO_3, i.e., total nitrite (NOx), the stable oxidative products of NO, were measured in placenta and serum samples using the Griess reagent system [5].

Total Antioxidant Capacity Assay

Total antioxidant capacities (TACs) of placenta or serum samples were measured with a TAC assay kit following the manufacturer's instructions (Beyotime Biotech Inc., Jiangsu, China).

Reverse Transcription and Real-Time Quantitative Polymerase Chain Reaction

For gene expression analysis, total RNA was isolated from placenta tissues with TRIzol reagent (Invitrogen, Carlsbad, CA) according to the manufacturer's protocols, and a total of 1 μg RNA was reverse-transcribed into complementary DNA (cDNA) using the ReverTra Ace qPCR RT Master Mix with gDNA Remover system (Toyobo, Japan). Real-time quantitative polymerase chain reaction (qPCR) was performed with the iTaq™ Universal SYBR Green Supermix (Bio-Rad, USA) on the MiniOpticon™ detection system (Bio-Rad, USA). The 10 μl amplifying system was composed of the following elements: 5 μl iTaq™ Universal SYBR Green Supermix (1×), 0.5 μl sense primer (400 nM), 0.5 μl antisense primer (400 nM), 1 μl cDNA (100 ng), and 3 μl deionized water

(Ambion, USA). The cycling parameters were set up as follows: 95 °C, 30 s, for pre-denaturation; 95 °C, 30 s, for denaturation; and 60 °C, 30 s, for annealing and extension, 40 cycles. PCR primers were designed with the Primer 5.0 software and synthesized by Sangon Biotech Co., Ltd. (Shanghai, China). The sequences of primers tested are listed in Table 1. Specificity of amplification products was checked by the melting curve analysis. Densitometric analysis of the band was performed using Image J 1.46 software to normalize the expression of target gene with the corresponding housekeeping gene. The relative expression of each interested gene was calculated by the $2^{-\Delta\Delta Ct}$ method [6].

Western blot Analysis

Proteins were extracted using commercial protein extraction reagent (Pierce, Rockford, Illinois, USA). Protein concentrations were determined using a BCA protein assay kit (Pierce, Rockford, Illinois, USA). Then, equal amount of sample protein (40 μg) together with prestained protein Ladder (Fermentas, Canada) was separated by SDS-PAGE, followed by transfer onto nitrocellulose membranes (Pall, USA) or polyvinylidene difluoride membranes (Millipore, Billerica, MA, USA). The membranes were blocked in TBS-T (Tris-buffered saline with 0.1 % Tween 20) containing 5 % BSA and probed with specific primary antibodies, including anti-apurinic/apyrimidinic endonuclease 1 (APE1) (1:10,000; Abcam, Cambridge, MA, USA), anti-p53 (1:1000; Abcam, Cambridge, MA, USA), anti-β-Actin (1:1000; Abcam, Cambridge, MA, USA), anti-histone deacetylase 1 (HDAC1) (1:1000; Abcam, Cambridge, MA, USA), anti-nuclear factor erythroid 2-related factor-2 (Nrf-2) (1:1000; Sangon, Shanghai, China), anti-superoxide dismutase 1(SOD1, Cu/Zn-SOD) (1:1000; Sangon, Shanghai, China), anti-glutathione reductase (GR) (1:1000; Sangon, Shanghai, China), anti-thioredoxin (TRX) (1:1000; Sangon, Shanghai, China), anti-GAPDH (1:2000; Sangon, Shanghai, China), and anti-HIST1H3A (H3/A) (1:1000; Sangon, Shanghai, China) overnight at 4 °C. The membranes were washed three times, followed by incubation with horseradish peroxidase (HRP)-conjugated secondary antibodies for 1 h at room temperature. Then, protein bands were visualized by enhanced chemiluminescence detection reagents (Pierce, Rockford, Illinois, USA), and densitometric analysis was performed using ImageJ 1.46 software to normalize the expression of target protein with the corresponding loading control.

Immunohistochemistry Assay

Paraffin sections (4 μm) from 4 % paraformaldehyde-fixed tissues were dewaxed in xylene and rehydrated in descending grades of ethanol. Antigen retrieval was carried out by microwave heat treatment in citrate buffer (0.01 M, pH 6). Endogenous peroxidase activity was blocked in 3 % hydrogen peroxide (H_2O_2) solution. After washing with PBS for three times, sections were blocked with 3 % blocking serum for 30 min at room temperature, followed by incubation with anti-8-hydroxy-2′-deoxyguanosine (8-OHdG) (1: 100; Abcam, Cambridge, MA, USA) or anti-APE1 (1: 100; Abcam, Cambridge, MA, USA) antibody overnight at 4 °C. Then, sections were incubated with HRP-conjugated secondary antibodies for 60 min at room temperature, followed by application of diaminobenzidine solution. Sections were counterstained with Harris hematoxylin. Negative controls were run in parallel by replacing the primary antibodies with non-immune immunoglobulins from the same species of primary antibodies, while blank controls were performed with PBS instead of the primary antibodies. Immunoreactivity was identified under a light microscope (Olympus BX60, Japan) linked to a digital camera (Nikon, Japan). More than 1000 nuclei from each group were randomly examined, with 8-OHdG or APE1 positive nuclei being counted. Then, the proportion of targeted nuclei was calculated as the positively stained nuclei number/total nuclei number.

Statistics

SPSS 19.0 software was used to perform the statistical analyses. Unless stated otherwise, all data were expressed as mean ± SEM of at least three independent experiments performed in triplicate. A t test or one-way analysis of variance (ANOVA) followed by a least significant difference (LSD)-t test or Dunnett T3 test was performed to compare means of different experimental groups if the data were normally distributed, while a non-parametric test (Mann–Whitney U test or Kruskal-Wallis H test) was applied to determine the statistical differences for the non-normal distributed data. Differences were considered statistically significant at $p < 0.05$.

Table 1 Sequences of primers used in RT-qPCR

Target mRNA	Prime	Sequence
Ape1	Forward	5′-CCCGCTCTAAGAATGTTGGTTG-3′
	Reverse	5′-CAGTGCTAGGTAAAGGGTGATGG-3′
p53	Forward	5′-CCCATCCTTACCATCATCAC-3′
	Reverse	5′-CAGGCACAAACACGAACC-3′
β-Actin	Forward	5′-CGTTGACATCCGTAAAGACC-3′
	Reverse	5′-TAGGAGCCAGGGCAGTAATC-3′

Results

Effects of CdCl$_2$ on Maternal and Fetal General Conditions

The characteristics of rats subjected to different doses of Cd are described in Fig. 1. The dose of 0.25 Cd had no obvious effect on maternal body weight, while the dose of 0.5 Cd slowed its growth rate with less gain ($p < 0.05$; Fig. 1a). PE is a specific pregnancy-associated disease characterized by the new-onset hypertension and proteinuria after 20 weeks of human gestation. The average SBPs of the control and NP groups did not change significantly during the whole experimental periods. However, Cd-treated pregnant rats had their SBPs rocketed on GD 11 and 18, with increased urinary albumin excretion on GD 20 ($p < 0.01$; Fig. 1b, c).

Furthermore, morphological changes in placentae and kidneys from 0.25 Cd-treated pregnant rats were examined under a light microscope. HE staining showed normal microstructures of placentae from control group, which indicated a normal thickness of placental vascular walls with smooth intimae, no obvious lumen stenosis, and rare inflammatory cells (Fig. 1d (d1, d2)). However, placentae from 0.25 Cd group presented thickened vessel walls, rough vascular intimae with narrowed vessel lumens, and a large number of infiltrated inflammatory cells (Fig. 1d (d3, d4)). Figure 1e (e1, e2) presented the normal appearance of glomeruli with clearly seen Bowman's space of control group. However, CdCl$_2$ infusion caused microstructural alterations in kidney tissue characterized by glomerular endothelial cell hyperplasia with narrowed Bowman's space and infiltrated inflammatory cells (Fig. 1e (e3, e4)).

The developmental evaluations of fetuses and placentae were summarized in Table 2. The fetal growth and development of 0.5 Cd group was the poorest among the other two pregnant groups. Each dam from 0.5 Cd group had one or
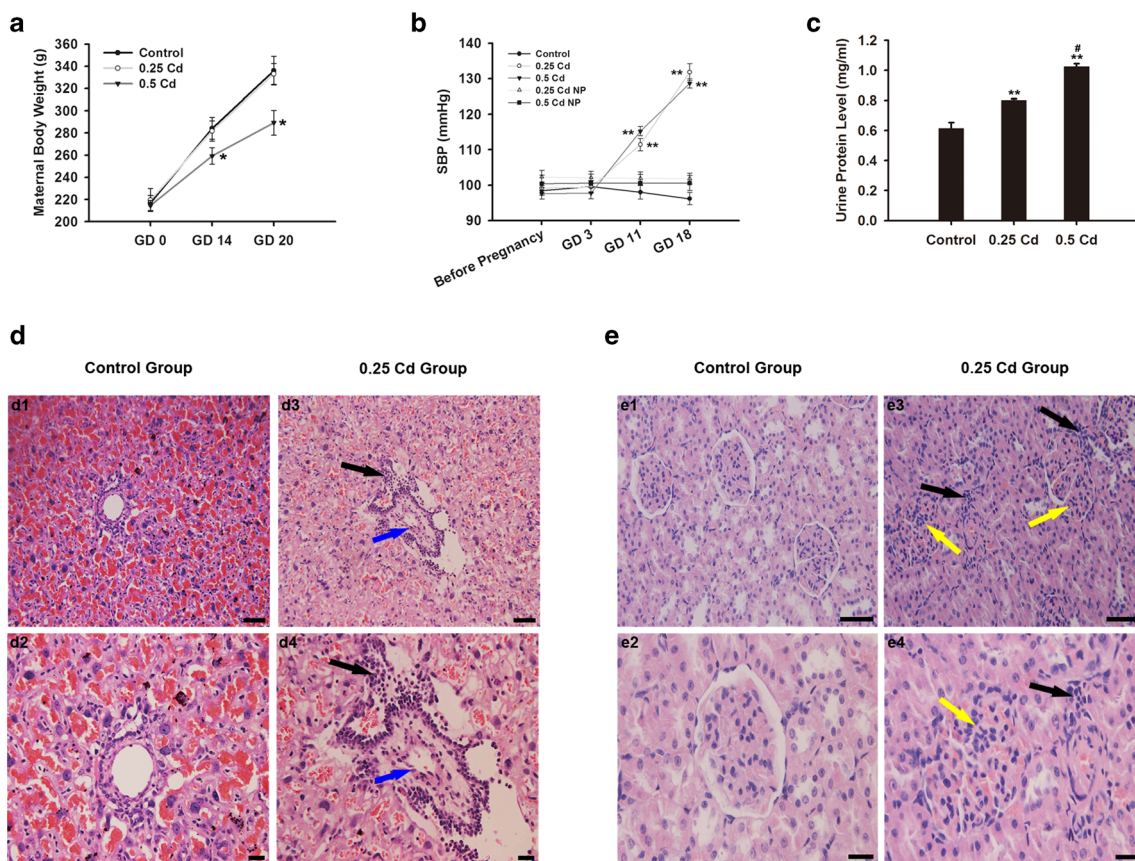

Fig. 1 Effects of CdCl$_2$ on maternal and fetal general conditions. **a** Maternal body weight was measured on GD 0, 14, and 20. **b** SBPs of rats. **c** Urine protein levels of pregnant rats. All data were expressed as mean ± SEM. *$p < 0.05$ versus 0.25 Cd and control groups (**a**); **$p < 0.01$ versus before pregnancy and GD 3 of the corresponding group, or versus control and NP groups at the same time points (**b**); **$p < 0.01$ versus control group, #$p < 0.01$ versus 0.25 Cd group (**c**).

Effects of CdCl$_2$ on placenta (**d**) and kidney (**e**) morphological features of pregnant rats. The magnifications were ×200 (*d1, d3, e1, e3; scale bar = 50 μm*) and ×400 (*d2, d4, e2, e4; scale bar = 20 μm*), respectively. *Black arrows* indicated the numerous infiltrated inflammatory cells. *Blue arrows* indicated the rough intimae of placental blood vessels. *Yellow arrows* indicated glomerular endotheliosis

Table 2 Developmental parameters of fetuses and placentae (mean ± SEM)

Group	Number of placentae	Number of live fetuses	Number of dead fetuses	Placental weight (g)	Fetal weight (g)
Control ($n = 10$)	13.00 ± 0.63	13.00 ± 0.63	0	0.50 ± 0.01	3.81 ± 0.09
0.25 Cd ($n = 10$)	10.80 ± 0.73	10.20 ± 0.80*	0.60 ± 0.43	0.51 ± 0.03	3.28 ± 0.31
0.5 Cd ($n = 8$)	10.13 ± 1.27	6.50 ± 1.44**	3.63 ± 1.12[#]	0.43 ± 0.06	2.47 ± 0.36*

*$p < 0.05$ versus control group, **$p < 0.01$ versus control group, [#] $p < 0.01$ versus 0.25 Cd group

more dead pups; the average number of live fetuses was significantly decreased than that of control group ($p < 0.01$) accompanied by a lower birth weight ($p < 0.05$). And the average number of live fetuses of 0.25 Cd group was also reduced than that of control group ($p < 0.05$), but the mean number and weight of placentae showed no statistical difference among the three groups ($p > 0.05$). It seemed that prenatal Cd exposure affected the growth and development of the off-springs independent of the placentae.

Cadmium Concentration in Maternal Blood

Cd level in the blood of 0.5 Cd group (31.4 ± 0.1 μg/L) was significantly higher than that of 0.25 mg/kg Cd-treated group (15.1 ± 0.2 μg/L). The blood Cd level of the control group was below the detectable limit.

Effects of CdCl$_2$ on Maternal Redox Balance

CdCl$_2$ Increased Maternal NOx Production in Serum and Placenta Tissue

NOx is often regarded as a biomarker of oxidative stress, its content in the body indirectly reflects the level of NO [7]. As a reactive oxygen species (ROS) and reactive nitrogen species (RNS) inducer, CdCl$_2$ increased NOx generation in serum and placenta tissue of pregnant rats ($p < 0.01$; Table 3).

CdCl$_2$ Abated the TACs of Serum and Placenta Tissue

The organism is orchestrated with a battery of antioxidative factors, including enzymatic and non-enzymatic antioxidants to neutralize the harmful free radicals. And the sum of antioxidant activities of this "nonspecific" pool of antioxidative components reflects the total antioxidant capacity of the

system [8]. Table 3 indicated that TAC of serum or placenta tissue was weakened by CdCl$_2$ injection.

CdCl$_2$ Up-regulated the Levels of GR, TRX, SOD1, and Nrf-2 in Placenta Tissue

GR, TRX, and SOD1 are all the antioxidants that equipped in the body to battle against oxidative stress. As free radical scavengers, GR, TRX, and SOD1 play very important roles in eliminating kinds of ROS and RNS induced by Cd and maintain the redox balance [9–11]. And as a transcription factor, Nrf-2 regulates the transcription of its downstream antioxidant (such as CAT, TRX) or phase II detoxifying enzyme genes [12], thus protecting cells from oxidative stress or other toxic substances [13–15]. Western blot depicted that CdCl$_2$ notably up-regulated the expression levels of GR, TRX, SOD1, and Nrf-2 protein in placenta tissue (**$p < 0.01$; Fig. 2).

Effects of CdCl$_2$ on the Oxidative DNA Damage/Repair Pathway in Placenta

CdCl$_2$ Increased the Generation of 8-OHdG in Placenta Tissue

As a stable metabolite, 8-OHdG is exclusively formed via the oxidative DNA damage pathway, and its content in body fluid is not interfered by daily diets or other factors. Therefore, 8-OHdG is internationally recognized as a novel and sensitive biological indicator for oxidative DNA damage and oxidative stress evaluations [16]. Immunohistochemistry showed that 8-OHdG was expressed in the nuclei of placental cells in both control and 0.25 Cd groups. However, the percentage of 8-OHdG positive nuclei in CdCl$_2$-treated placentae was strikingly higher than that of control group ($p < 0.05$; Fig. 3a).

Table 3 NOx level and TAC of serum or placenta tissue (mean ± SEM)

Group	Serum		Placenta	
	NOx (μmol/l)	TAC (mmol/l)	NOx (μmol/g protein)	TAC (mmol/g protein)
Control	2.18 ± 0.22	0.74 ± 0.16	1.45 ± 0.04	0.17 ± 0.01
0.25 Cd	5.54 ± 0.97**	0.30 ± 0.01*	1.91 ± 0.07**	0.08 ± 0.01**

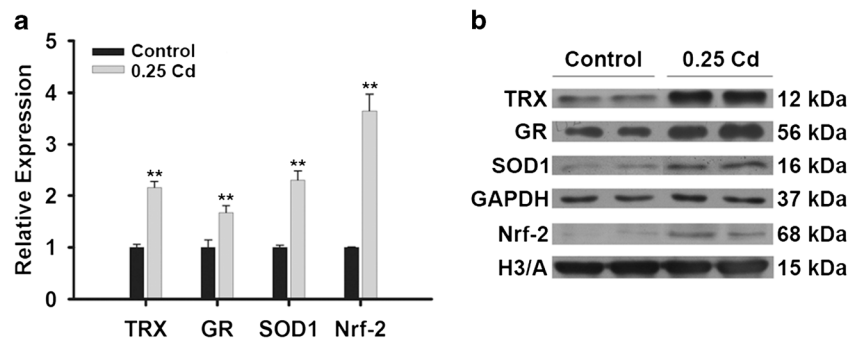*$p < 0.05$ versus control group, **$p < 0.01$ versus control group

Fig. 2 Effects of CdCl$_2$ on placenta GR, TRX, SOD1, and Nrf-2 protein levels in pregnant rats. **a** Western blot analyses of GR, TRX, and SOD1 levels in placental total protein extractions with GAPDH served as the loading control and Nrf-2 expression in nuclear protein with H3/A served as the loading control. **b** Densitometric analyses of the bands were performed using ImageJ 1.46 software to normalize GR, TRX, and SOD1 expressions with the corresponding GAPDH level, while Nrf-2 with H3/A, and the results were presented as the relative expression of control group. Data shown were representative of three independent experiments and expressed as mean ± SEM. **p < 0.01 versus control group

CdCl$_2$ Promoted the mRNA and Protein Levels of APE1 and p53 in Placenta

In order to detect whether CdCl$_2$ affected placental DNA repair system of pregnant rats, we chose two typical molecular markers of DNA damage/repair pathway—APE1 [17] and p53 [18, 19]—as our observational indexes and determined their expressions at both the mRNA and protein levels. RT-qPCR and western blot suggested much stronger signals for APE1 and p53 in placenta tissues of 0.25 Cd group (Fig. 3b–f). Moreover, our immunohistochemistry indicated a major cellular location of APE1 in the nuclei of trophoblasts, and APE1 positive nuclei was more frequently found in CdCl$_2$-administrated placentae (p < 0.05; Fig. 3g).

Discussion

Oxidative stress is now commonly regarded as an imbalanced state between pro-oxidation and antioxidation with the former being the dominating force, which results in an accumulation of free radical compounds [20]. Normal pregnancy is a process of slight oxidative stress, to some extent. However, excessive oxidative stress could result in pathological pregnancy. Cd is a bivalent transition element with a relatively weak reducing capacity, which cannot produce free radicals directly. However, a considerable number of studies have described that exposure to Cd could lead to oxidative stress, although the potential mechanisms are still unclear [21].

In the present study, we found CdCl$_2$ increased NOx generation in serum and placenta tissue of pregnant rats. As a marker of oxidative stress, NOx indirectly reflects the level of NO in the body [7]. On one hand, as a benign and potent vasodilator, NO participates in vascular dilatation, and its poor generation has a close relationship with hypertension in PE individuals [22]. However, Palmer et al. indicated that an excess of NO in itself may also damage the vascular

endothelium, which is associated with the occurrence of PE [23]. Therefore, as an evil, on the other hand, NO, together with other free radicals, contributed to the potential oxidative stress in the presence of the transition metal Cd [24].

We also detected the systemic and local antioxidant abilities in our experimental animals. It seemed that the decreased total antioxidant capacity was contradictory with the compensatorily incremental levels of GR, TRX, SOD1, and Nrf-2 in CdCl$_2$-treated rats. We supposed that, despite of the huge quantities of the antioxidant-related factors, the qualities of these beneficial proteins were degraded by the heavy metal Cd, which mean the bioeffects of these antioxidants and the DNA-binding ability of Nrf-2 were weakened. Ferramola et al. revealed that the enzymatic activities of antioxidants could be modified by Cd^{2+} [25]. We speculated that Cd^{2+} probably interfered or inactivated the biological functions of those proteins (e.g., Zn/Cu-SOD) by replacing the essential elements in the functional domains of their molecular structures or disturbing the metabolisms of metal ions which were

Fig. 3 Effects of CdCl$_2$ on placenta DNA repair/damage biomarkers in pregnant rats. **a** The presence of 8-OHdG in the nuclei of placental cells was detected by immunohistochemistry. The magnifications were ×200 (a1–a4, scale bar = 50 μm) and ×400 (a5–a8, scale bar = 20 μm), respectively. *Black arrows* indicated the negatively stained nuclei; *red arrows* indicated the positively stained nuclei. **b** Placental APE1 and p53 mRNA levels were analyzed by RT-qPCR and normalized to the housekeeping gene β-Actin. The data were presented as the relative expression of control group. Western blot analyses of APE1 and p53 expressions in placental cytoplasmic (**c**) and nuclear extractions (**e**). β-Actin and HDAC1 were served as the cytoplasmic and nuclear protein loading control, respectively. **d, f** Densitometric analyses of the bands in (**c**) and (**e**) were performed using ImageJ 1.46 software to normalize APE1 and p53 expression with the corresponding loading control level and presented as the relative expression of control group. Data shown were representative of three independent experiments and expressed as mean ± SEM. *p < 0.05 or **p < 0.01 versus control group. **g** Immunohistochemistry showed that APE1 primarily appeared in the nuclei of placental trophoblasts. The magnifications were ×200 (g1–g4, scale bar = 50 μm) and ×400 (g5–g8, scale bar = 20 μm), respectively. *Black arrows* indicated the negatively stained nuclei; *red arrows* indicated the positively stained nuclei
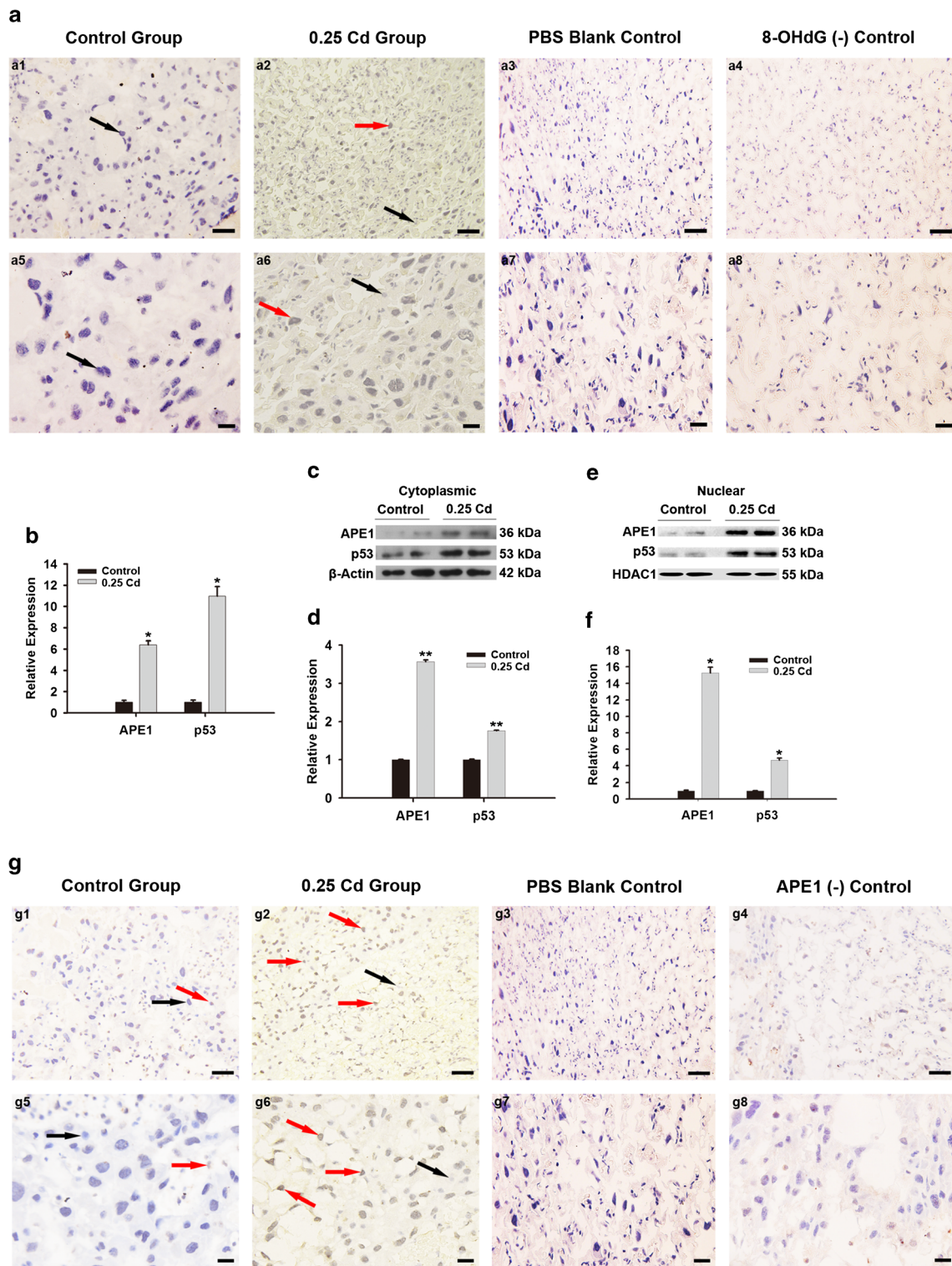
indispensable for the enzymatic activities to effect. So, with this point in mind, despite of the quantitatively overwhelming antioxidative forces, the organism, in essence, was still in a state of oxidative stress. What was worse, in the absence of efficient antioxidant activities, NO might react with superoxide to produce a harmful nitric free radical, peroxynitrite ($ONOO^-$), leading to lipid peroxidation [24, 26]. Thus, $CdCl_2$ promoted oxidative activities and impaired the antioxidant system at the same time, resulting in oxidative stress.

There is substantial evidence to suggest that oxidative stress provokes extensive damages to the macromolecular substances, involving protein degradation, oxidative DNA damage, and lipid peroxidation [21]. There are reports on the oxidative DNA damage in preeclamptic pregnancies, although the biological importance remains to be determined. In our immunohistochemistry study, we observed that $CdCl_2$ aggravated oxidative DNA damage in pregnant rats, indicated by a higher proportion of 8-OHdG positive nuclei in placenta tissue. It was reasonable to infer that such DNA damage would disturb the well-functioning of placenta (such as trophoblastic invasion, placentation) at gene transcriptional levels, therefore, contributing to the pathogenesis of PE.

In our research, we also discovered that several DNA repair factors which are involved in base excision repair (APE1) or nonspecific repair pathways (p53) were remarkably increased, both at gene and protein levels. Changes in the expression levels of these repair components are usually adopted as useful clues for evaluating the severity of oxidative stress or oxidative DNA damage [15]. Overexpression of some repair enzymes does not always contribute to enhanced protection against DNA-damaging agents [27]. In this regard, it waits to be seen whether the capacity or efficiency of Cd-treated placenta to repair DNA lesions after up-regulation of specific repair elements is improved. An excess of certain repair proteins may even prove detrimental more than beneficial to mammalian cells [27].

In summary, our findings display that pregnant rats exposed to Cd successfully develop the phenotypic characteristics of human preeclampsia (e.g., hypertension, proteinuria). We demonstrate that increased oxidative DNA damage in placenta contributes to the development of preeclamptic conditions in rat. However, currently, there has been a lack of enough knowledge explaining the functional consequences of damaged DNA in preeclamptic placenta. And the role of DNA repair is not very well understood in preeclampsia, nor, indeed, in normal pregnancy, further investigations will no doubt be needed.

References

1. Young BC, Levine RJ, Karumanchi SA (2010) Pathogenesis of preeclampsia. Annu Rev Pathol 5:173–192
2. Roberts JM, Cooper DW (2001) Pathogenesis and genetics of preeclampsia. Lancet 357:53–56
3. Lucian B, Camelia B, Vasile B, Otilia M, Mariana M (2010) Report on the influence of heavy metals on the evolution of the pregnancy in smoking mothers. Analele Universităţii din Oradea Fascicula: Ecotoxicologie, Zootehnie si Tehnologii de Industrie Alimentară 99–104.
4. Helmestam M, Stavreus-Evers A, Olovsson M (2010) Cadmium chloride alters mRNA levels of angiogenesis related genes in primary human endometrial endothelial cells grown in vitro. Reprod Toxicol 30:370–376
5. Ling Y, Ye X, Ji H, Zhang YH, Lai YS, et al (2010) Synthesis and evaluation of nitric oxide-releasing derivatives of farnesylthiosalicylic acid as anti-tumor agents. Bioorg Med Chem 18:3448–3456
6. Livak KJ, Schmittgen TD (2001) Analysis of relative gene expression data using real-time quantitative PCR and the $2^{-\triangle\triangle Ct}$ method. Methods 25:402–408
7. Pistarini C (2013) Oxidative stress in post-acute ischemic stroke patients: relevance of early intensive neurorehabilitation. J Neurol Neurophysiol 4:154
8. Bartosz G (2003) Total antioxidant capacity. Adv Clin Chem 37: 220–292
9. Mitra E, Ghosh AK, Ghosh D, Mukherjee D, Chattopadhyay A, Dutta S, et al (2012) Protective effect of aqueous curry leaf (Murraya koenigii) extract against cadmium-induced oxidative stress in rat heart. Food Chem Toxicol 50:1340–1353
10. Nair A, DeGheselle O, Smeets K, Van Kerkhove E, Cuypers A (2013) Cadmium-induced pathologies: where is the oxidative balance lost (or not)? Int J Mol Sci 14:6116–6143
11. Wang Q, Ning X, Chen L, Pei D, Zhao J, Zhang L, et al (2011) Responses of thioredoxin 1 and thioredoxin-related protein 14 mRNAs to cadmium and copper stresses in venerupis philippinarum. Comp Biochem Physiol C Toxicol Pharmacol 154: 154–160
12. Zhang M, An C, Gao Y, Leak RK, Chen J, Zhang F (2013) Emerging roles of Nrf2 and phase II antioxidant enzymes in neuroprotection. Prog Neurobiol 100:30–47
13. Mann GE, Niehueser-Saran J, Watson A, Gao L, Ishii T, de Winter P, et al (2007) Nrf2/ARE regulated antioxidant gene expression in endothelial and smooth muscle cells in oxidative stress: implications for atherosclerosis and preeclampsia. Sheng Li Xue Bao 59: 117–127
14. Lin F, Yu X, Zhang X, Guo Y, Huang Y, Zhou J, et al (2013) A synthetic analog of lipoxin A4 partially alleviates dexamethasone-induced fetal growth restriction in rats. Placenta 34:941–948
15. Storr SJ, Woolston CM, Zhang Y, Martin SG (2013) Redox environment, free radical, and oxidative DNA damage. Antioxid Redox Signal 18:2399–2408
16. Kasai H (1997) Analysis of a form of oxidative DNA damage, 8-hydroxy-2'-deoxyguanosine, as a marker of cellular oxidative stress during carcinogenesis. Mutat Res Rev Mutat Res 387:147–163
17. Kelley MR, Georgiadis MM, Fishel ML (2012) APE1/Ref-1 role in redox signaling: translational applications of targeting the redox function of the DNA repair/redox protein APE1/Ref-1. Curr Mol Pharmacol 5:36–53
18. Ho E, Ames BN (2002) Low intracellular zinc induces oxidative DNA damage, disrupts p53, NF κB, and AP1 DNA binding, and affects DNA repair in a rat glioma cell line. Proc Natl Acad Sci U S A 99:16770–16775
19. Hossain MZ, Gilbert SF, Patel K, Ghosh S, Bhunia AK, Kern SE (2013) Biological clues to potent DNA-damaging activities in food and flavoring. Food Chem Toxicol 55:557–567
20. Burton GJ, Jauniaux E (2011) Oxidative stress. Best Pract Res Clin Obstet Gynaecol 25:287–299
21. Cuypers A, Plusquin M, Remans T, Jozefczak M, Keunen E, Gielen H, et al (2010) Cadmium stress: an oxidative challenge. Biometals 23:927–940
22. Dai B, Liu T, Zhang B, Zhang X, Wang Z (2013) The polymorphism for endothelial nitric oxide synthase gene, the level of nitric

oxide and the risk for pre-eclampsia: a meta-analysis. Gene 519: 187–193

23. Palmer R, Bridge L, Foxwell N, Moncada S (1992) The role of nitric oxide in endothelial cell damage and its inhibition by gluco-corticoids. Br J Pharmacol 105:11–12

24. Siddiqui IA, Jaleel A, Tamimi W, Al Kadri HM (2010) Role of oxidative stress in the pathogenesis of preeclampsia. Arch Gynecol Obstet 282:469–474

25. Ferramola ML, Antón RI, Anzulovich AC, Giménez MS (2011) Myocardial oxidative stress following sub-chronic and chronic oral cadmium exposure in rats. Environ Toxicol Pharmacol 32:17–26

26. Gonenc A, Hacisevki A, Tavil Y, Cengel A, Torun M (2013) Oxidative stress in patients with essential hypertension: a comparison of dippers and non-dippers. Eur J Intern Med 24:139–144

27. Frosina G (2000) Overexpression of enzymes that repair endogenous damage to DNA. Eur J Biochem 267:2135–2149